NEW DESIGN OF A COLLIMATOR SYSTEM AT THE PSI PROTON ACCELERATOR

Y. Lee*, D. Reggiani, M. Gandel, D. C. Kiselev, P. Baumann, M. Seidel,
A. Strinning, S. Teichmann, PSI, Villigen, Switzerland

Abstract

PSI is gradually upgrading the 590 MeV proton beam intensity from the present 2.2 mA towards 3 mA, which poses a significant challenge to the reliable operation of the accelerator facility. Of particular concern is the collimator system which is exposed to the strongly divergent beam from a muon production target. It shapes an optimal beam profile for low-loss beam transport to the neutron spallation source SINQ. The current collimator system absorbs about 14 % of the proton beam power. Consequently, the maximum temperature of the collimator system exceeds 400 C at 2.2 mA, which is close to the limit set for safe operation. In this paper, we present a new collimator system design which could withstand the proton beam intensity of 3 mA, while fulfilling the intended functionality. Advanced multiphysics simulation technology is used for the geometric and material optimizations, to achieve the lowest possible actual to yield stress ratio at 3 mA. A sensitivity study is performed on the correlation between the beam misalignments and the reliability of the accelerator components in the proton downstream region.

INTRODUCTION

The ring cyclotron at PSI generates 590 MeV proton beam with the beam current up to 2.3 mA. The protons are guided to collide with solid targets, in order to generate high flux muons and neutrons for various research purposes. Figure 1 shows the beamline elements at the PSI proton accelerator between the 4 cm thick graphite muon generation target (Target E) and the bending magnet (AHL).

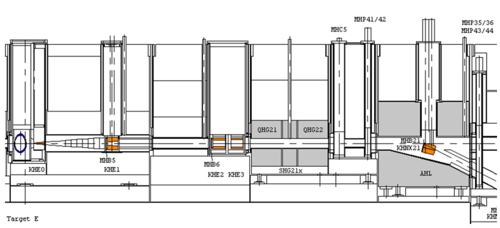

Figure 1: The beamline elements at the PSI proton accelerator between the muon generation target (Target E) and the bending magnet (AHL). The Q21 and Q22 are quadrupole magnets.

As the proton beam hits Target E, it diverges via elastic and inelastic Coulomb scatterings. While the scattered secondary particles are absorbed by the two collimators KHE0 and KHE1, the divergent direct beam must be collimated by the collimator system composed of KHE2 and KHE3. This is to protect the accelerator components and the proton channel between Target E and the neutron production target SINQ.

The collimator system composed of KHE2 and KHE3 is made of OFHC copper and absorbs approximately 14 % of the total proton beam power. In 2009, 1.3 MW (590 MeV/2.3 mA) proton beam power was routinely used at PSI. The thermal load which the collimator system must sustain is then close to 200 kW. The maximum temperature is estimated to reach up to 700 K (430 C) which is about 50 % of the melting temperature of the OFHC-copper. The planned proton beam intensity upgrade at PSI therefore poses a significant challenge to the stable operation of the accelerator facilities, due to the enhanced thermal load from proton beam stopping at the collimator system. In this paper, we propose a collimator design which further optimizes the basic design concept presented in Ref. [1], which could sustain the thermal load from the planned 1.8 MW (590 MeV/3.0 mA) beam upgrade.

WORKING PRINCIPLES

A quarter model of the present collimator system composed of KHE2 and KHE3 is shown in Fig. 2. The collimator system must stop the 590 MeV protons completely, which would otherwise directly hit the accelerator components behind. Therefore, it should be longer than the projected stopping range of a 590 MeV proton in copper, which is calculated to be 25 cm by MCNPX [2]; see Fig. 3. The KHE2 reduces the beam power before the protons impinges on KHE3, and the final collimation is done in KHE3. In order to remove the beam stopping power from the collimator, active water cooling through brazed stainless steel pipes is applied. The KHE2 is exposed to higher

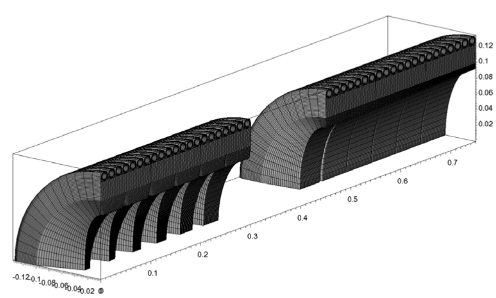

Figure 2: A quarter of the collimator system model: The KHE2 (left) at the beam entry side and the KHE3 at the beam exit side (right).

* yong-joong.lee@psi.ch

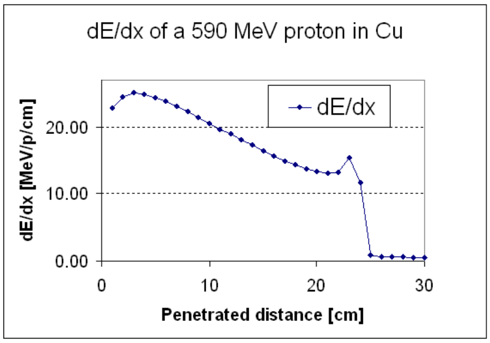

Figure 3: Differential stopping power of a 590 MeV proton in copper.

heat load from proton beam energy deposition than KHE3, which necessitates more careful thermal design. The KHE2 is composed of 6 teeth like structure; see Fig. 2. Along the beam direction, the width of the tooth increases. This is to distribute the thermal load uniformly along the axial direction, as the differential proton stopping power decreases as it travels through copper; see Fig. 3. The aperture gets larger in accordance with the beam divergence. The KHE3 is composed of six uniform teeth, each with approximately 5 cm thickness. This makes the total travel length of the to be absorbed protons larger than the projected stopping range of 25 cm.

SENSITIVITY ANALYSIS REGARDING COLLIMATOR APERTURE SIZE

Beam Dynamics Aspects

The further opening of the collimator aperture should reduce the thermal load and allow longer life time of the collimator system. In addition, it transmits more beam power to SINQ which should lead to an enhanced neutron flux. But, it could also result in unacceptable thermal load on accelerator components between the collimator system and the SINQ. In order to know the balance point between these two contradictory aspects, a number of simulations has been performed using the ray tracing program TURTLE [3].

For TURTLE calculations, a simplified collimator geometry is used. The collimator system is modeled with two cylinder blocks with conic aperture. The length of each collimator is modified, according to the travel range of the proton beam through the teeth-like structure. Shown in Fig. 4 is the parametrization of the KHE2 of the elliptic aperture. The opening of the present KHE2 at the beam entry side is described by an ellipse with the vertical major axis $a = 160$ mm and the horizontal minor axis $a/2 = 80$ mm. The parameter x represents the change in aperture, which is used for sensitivity study.

Figure 5 shows the correlation between the aperture opening and the beam losses at the accelerator magnets located up to 10 m downstream of the collimator system. As

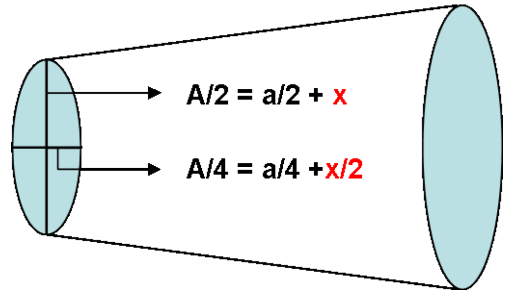

Figure 4: Model geometry parametrization used for TURTLE ray tracing simulations.

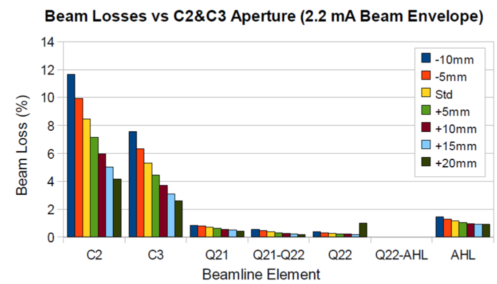

Figure 5: Beam losses for different collimator apertures at the beamline elements up to the bending magnet AHL which directs the proton beam towards SINQ.

the aperture opens up from $x = 0$ mm, the beam losses at the accelerator components decreases until the x parameter exceeds 20 mm. This is due to the reduced level of multiple Coulomb scattering at KHE2 and KHE3, for larger apertures. For $x \geq 20$ mm, the simulation shows that the beam particles get directly lost onto the quadrupole magnet Q22. Taking engineering safety margin into account, a realizable optimal collimator aperture can be achieved for the opening parameter $x = 10$ mm.

Thermal Load Aspects

Particle transport codes based on Monte-Carlo (MC) methods such as MCNPX [2] are commonly used for proton beam stopping power calculations in accelerator components. However, MC power deposition simulations for a complicated component like the collimator system needs large particle statistics. This makes it computationally expensive, particularly for design optimization study where many numbers of geometry parameters are involved. For this reason, a FORTRAN 90 code has been developed, which calculates the volumetric heat source from the proton beam stopping. This FORTRAN code is coupled to multiphysics simulation tool CFD-ACE+ [4], for thermal and mechanical calculations.

The beam stopping power calculating routine is based on the approximation that the proton scatters with '*zero*' angle. This approximation is based on the physical picture that, in each Coulomb interaction in copper, an energetic proton loses a small amount of kinetic energy and experiences a small angle scattering [5]. The basic inputs to the routine are the proton beam directional vector, the grid connectivity information, the differential proton power loss and the proton beam current density distribution. As an output, it generates volumetric power source in W/m^3 at each mesh cell for thermal and mechanical simulations; see Ref. [1] for details. The calculated proton power deposition obtained from the FORTRAN code is verified with a MCNPX calculation [1]. These two results agree within 20 % and the difference comes from the fact that the FORTRAN routine does not take the proton scatterings and secondary particle productions into account.

We study the influence of collimator aperture opening on the temperature field of the collimator system. Taken for the thermal calculations are the present collimator system and the one with 12.5 % larger aperture (the case with $x =$ 10 mm). The reference proton beam current is taken to be 2 mA. Figure 6 shows the calculated temperature fields of the current collimator system. The collimator system with

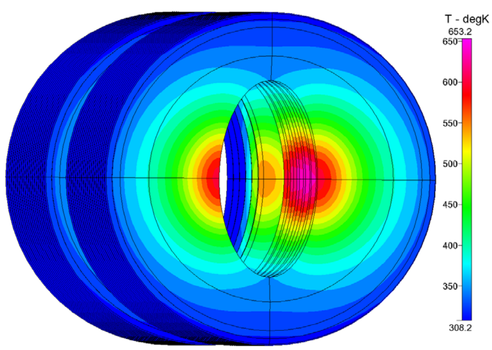

Figure 6: Calculated temperature field of the current collimator system at 2 mA.

larger aperture shows the similar temperature profiles as the present one, but with the peak temperature 552 K which is lower than 653 K of the present one by 81 K. This is due to the reduced heat load from the beam stopping in the collimator system. The calculated power depositions are 170 kW for the present one and 122 kW for the one with the larger aperture. These account for 14.4 % and 10.3 % of the 590 MeV/2.0 mA proton beam power, respectively.

SENSITIVITY ANALYSIS REGARDING BEAM MISALIGNMENTS

Beam Dynamics Aspects

The effect of beam misalignment has been studied with TURTLE simulations. Three different beam misalignments types are considered, for the collimator system with 12.5 % larger aperture: (1) Beam position mislocation at Target E [TE(x&y+2mm)], offset from the nominal beam location in the x (horizontal) and the y (vertical) direction by 2 mm each; (2) Beam angle misalignments at Target E [TE(xp&yp+2mrad)], offset in the x and the y direction by 2 mrad each; (3) KHE2 and KHE3 position and angle misalignments [C2(x& y+2mm,xp&yp+2mrad); C3(x& y+2mm,xp&yp+2mrad)], offset in the x and the y direction by 2 mm and 2 mrad each.

Figure 7 shows the calculated beam losses at the beamline elements located up to the bending magnet AHL, for different combinations of beam misalignments. The TURTLE simulations show that the beam loss profile is insensitive to beam position mislocation at Target E. The KHE2 misalignment does not produce noticeable additional losses, whereas the KHE3 misalignment affects the loss at the bending magnet AHL. The largest beam loss effect is seen from the beam angle misalignments at Target E. Nevertheless, sudden increase of beam losses at beamline elements after the collimator system is not expected from considered beam misalignments, even when the collimator aperture is widened by 12.5 %.

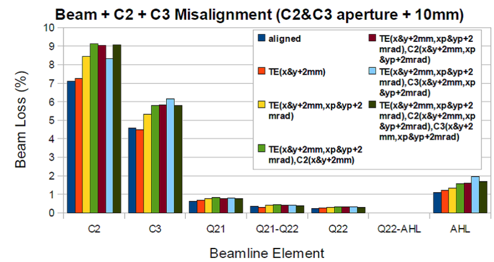

Figure 7: Beam losses at the beamline elements from KHE2 up to AHL, for different beam misalignments.

Thermal Load Aspects

The beam misalignments result in unbalanced temperature distribution in the collimator system. For the proton beam current 2 mA, thermal calculations have been performed using CFD-ACE+, coupled with FORTRAN user subroutine which calculates proton beam stopping power in copper. Two types of collimators are chosen for beam misalignment study. The present collimator system and the one with 12.5 % larger aperture. The following five scenarios of beam misalignments are chosen: (Misalignment type #1) Beam aligned; (Type #2) Beam position mislocation at Target E by 2 mm in the x direction [TE(x+2mm)]; (Type #3) Beam position mislocation at Target E by 2 mm in the y direction [TE(y+2mm)]; (Type #4) Beam angle misalignment at Target E by 1 mrad in the x direction [TE(xp+1mrad)]; (Type #5) Beam angle misalignment at Target E by 1 mrad in the y direction [TE(yp+1mrad)].

In order to quantify the beam misalignment effect, the collimator geometry is divided into four quadrants. The first quadrant is defined by the quarter geometry shown in Fig. 2, and the second, third and fourth quadrants are defined clockwise. Figure 8 shows the proton stopping power deposition in the 4 quadrants of the present KHE2, for considered beam misalignment types. The angular beam misalignment by 1 mrad in the x direction presents the worst case. The beam power deposited in the 2nd and the 3rd

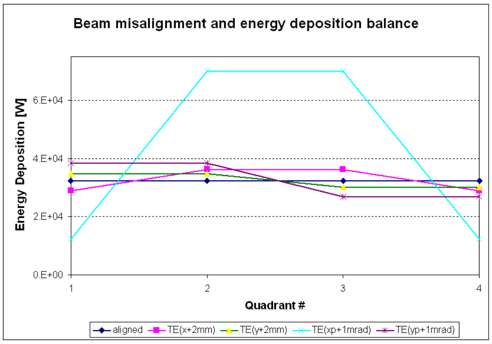

Figure 8: Beam stopping power deposition balance in the four quadrants of KHE2.

quadrants are factor 5.7 larger than that deposited in the first and the fourth quadrants. Figure 9 shows the temperature profiles of the present collimator system, for the worst beam alignment case. Clearly seen is the hot spot in the

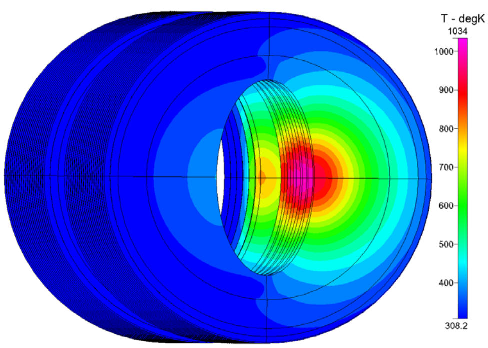

Figure 9: Temperature profile of the present collimator system for the angular beam misalignment [TE(xp+1mrad)].

2nd and the 3rd quadrants.

The thermal calculations show that the maximum temperature at the collimator system with larger aperture is significantly lower than that of the current one approximately by 100 K, for all studied misalignment types. The parameter study of different tilt angles for the collimator system with larger aperture shows that the peak temperature increases by less than 100 K from the nominal temperature 552 K, if the tilt angle is kept below 0.3 mrad. This means that the collimator system with larger aperture can tolerate additional angular beam misalignment of 0.3 mrad, compared to the present system. At 2 mA, it takes approximately 30 seconds for the maximum temperature to be increased by 100 K, which implies an additional time margin of 30 seconds before the interlock system activates.

OPTIMIZED COLLIMATOR

According to the sensitivity analysis on collimator aperture opening size, we further improve the thermal design of the collimator system presented in Ref. [1]. The guiding principle behind the optimization of the collimator design is the more balanced distribution of the thermal loads between KHE2 and KHE3. Figure 10 shows the 590 MeV single proton stopping power distributions in the current and the optimized collimator systems. Note that the proton is fully stopped at the third segment of KHE3 of the current collimator system. The last three segments are not used. On the other hand, the optimized collimator uses KHE3 more efficiently for beam stopping. The balance in

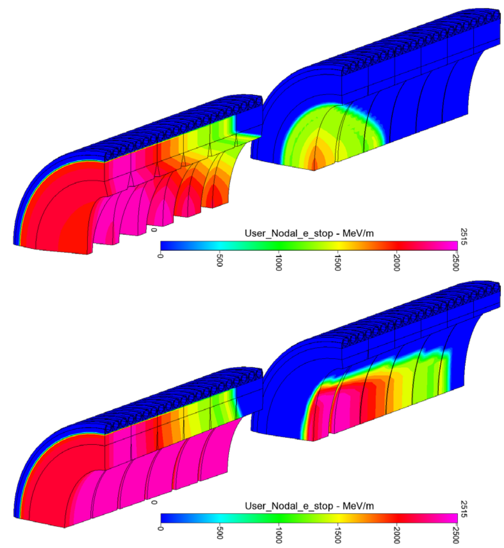

Figure 10: The 590 MeV single proton stopping power distributions in the current (top) and the optimized (bottom) collimator systems

deposited beam stopping powers between the KHE2 and KHE3 are listed in Table 1, for the three different collimator systems: (Type #0) The current collimator system; (Type #1) The collimator system with 12.5 % larger aperture; (Type #2) The optimized collimator system with convergent KHE2 and the divergent KHE3 apertures. Note that the thermal load is more uniformly distributed between KHE2 and KHE3 in the optimized collimator system.

Table 1: The Balance in Deposited Beam Stopping Powers Between the KHE2 and KHE3 at 3 mA

Type	KHE2 [kW/%]	KHE3 [kW/%]	Total [kW]
Type #0	197 (77%)	58 (23%)	255
Type #1	130 (71%)	53 (29%)	183
Type #2	128 (69%)	58 (31%)	186

The thermomechanical analysis of the optimized collimator poses some uncertainties regarding material data of OFHC copper. For fabrication of the collimator system, the water pipe which is made of stainless steel has to be brazed into the collimators. The reason why the cooling water cannot flow in the copper volume is that the water flow with the speed higher than 2 m/s causes erosion of the copper volume under beam irradiation [6]. The brazing process necessitates a heat treatment of the copper in a vacuum chamber at high temperatures between 600 C and 800 C. After the heat treatment at such high temperatures, the cold worked OFHC copper is known to lose most of the mechanical strength and becomes a soft non-linear material, as is confirmed by our tensile tests. For this reason, it is almost impossible to predict the thermomechanical characteristics of the collimator system made of OFHC copper, using numerical simulations.

An interesting candidate material for the next generation collimator is GLIDCOP® [7]. The preliminary analysis of our lab tests performed on GLIDCOP type AL-15 indicates that the GLIDCOP retains most of the mechanical strength after the heat treatment. The mechanical properties of the GLIDCOP for accelerator application can be found in Ref. [8]. thermomechanical simulations have been performed by CFD-ACE+, for the three types of collimator systems made of GLIDCOP AL-15. Figure 11 shows the calculated temperature and yield stress index profiles of the optimized collimator system, where the yield stress index is defined by the local von Mises stress divided by the local temperature dependent yield stress [1]. The peak temperatures and

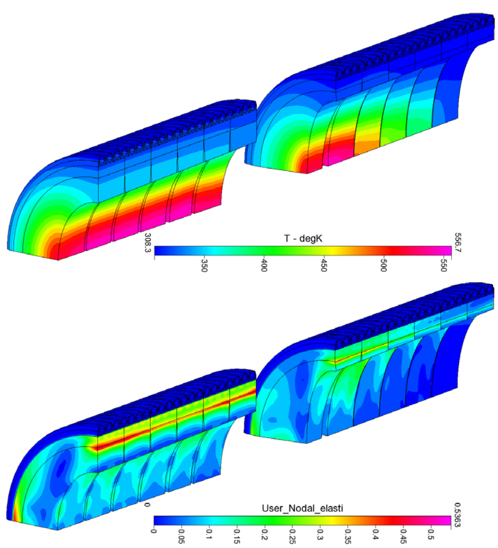

Figure 11: The calculated temperature (top) and yield index (bottom) profiles of the optimized collimator system for the proton beam current 3.0 mA.

the maximum yield stress indices of the three studied collimator types are listed in Table 2. The slightly higher maximum temperatures for the GLIDCOP option is due to its slightly lower thermal conductivity than the OFHC copper. The collimator system with 12.5 % larger aperture and the optimized convergent-divergent aperture collimator system shows the yield stress index below 1.0. This indicates a reliable operation of these two GLIDCOP collimator systems at 3 mA proton beam current.

Table 2: The maximum temperature and the maximum yield stress indices for three types of the collimator systems at 3 mA.

Type	Max. Temp. OFHC [K]	Max. Temp. GLIDC. [K]	Max. Yield Str. Index
Type #0	825.8	851.3	1.23
Type #1	674.3	692.3	0.67
Type #2	556.7	568.5	0.54

OUTLOOK

Still, there are uncertainties in the change of material properties of the OFHC copper and the GLIDCOP, under the proton beam irradiation. The relation between the dpa (displacement per atom) and the material properties of the GLIDCOP have been reported in a number of literature, mostly under the low energy neutron irradiations; see for example Ref. [9]. However, it is known that the dpa value lacks universality, and the material study based on the neutron irradiation cannot be directly applied to the material behavior under high energy proton irradiation. For this reason, two proton irradiation experiments are planned at PSI, in order to experimentally determine the material properties of the OFHC copper and the GLIDCOP. OFHC and GLIDCOP samples will be stationed in SINQ, within the framework of the SINQ Target Irradiation Program (STIP). Also considered is the implementation of the samples at the beam entry and exit regions of the collimator system. Once the uncertainties in material properties are solved, the detailed specifications of the collimator system will be determined.

REFERENCES

[1] Y. Lee et al, “Simulation based Optimization of a Collimator System for the Beam Current Upgrade at the PSI Proton Accelerator Facilities,” Proceedings of IPAC10, Kyoto, p. 4260 (2010).

[2] D. Pelowitz, ed., “MCNPX Users Manual,” Version 2.5.0, LA-CP-05-0369.

[3] U. Rohrer, “Graphic Turtle Framework,” `http://people.web.psi.ch/rohrer_u/turtle.htm`.

[4] CFD-ACE+, `http://www.esi-group.com`

[5] H. Frauenfelder and E.M. Henley, “Subatomic Physics,” 2nd. Ed., Prentice Hall, Upper Saddle River, New Jersey (1991).

[6] Gerd Heidenreich, Private communications.

[7] GLIDCOP is a registered trademark of SCM Metal Product Inc.

[8] R. Valdiviez, D. Schrage, F. Martinez and W. CLARK, “The Use of Dispersion-Strengthened Copper in Accelerator Designs,” Proceedings of XX International Linac Conference, Monterey, CA, p. 956 (2000).

[9] J.W. Davis and G.M. Kalinin, “Material properties and design requirements for copper alloys used in ITER,” J. of Nucl. Materials, Vols. 258-263, Part 1, p. 323-328 (1998).